

Article (refereed) - postprint

Liu, Yang; Baas, Jan; Peijnenburg, Willie J.G.M.; Vijver, Martina G. 2016.
Evaluating the combined toxicity of Cu and ZnO nanoparticles: utility of the concept of additivity and a nested experimental design.
Environmental Science & Technology, 50 (10). 5328-5337.
[10.1021/acs.est.6b00614](https://doi.org/10.1021/acs.est.6b00614)

© 2016 American Chemical Society

This version available <http://nora.nerc.ac.uk/514051/>

NERC has developed NORA to enable users to access research outputs wholly or partially funded by NERC. Copyright and other rights for material on this site are retained by the rights owners. Users should read the terms and conditions of use of this material at <http://nora.nerc.ac.uk/policies.html#access>

This document is the author's final manuscript version of the journal article, incorporating any revisions agreed during the peer review process. There may be differences between this and the publisher's version. You are advised to consult the publisher's version if you wish to cite from this article.

The definitive version is available at <http://pubs.acs.org/>

Contact CEH NORA team at
noraceh@ceh.ac.uk

1 **Evaluating the combined toxicity of Cu and ZnO nanoparticles:**
2 **utility of the concept of additivity and a nested experimental design**

3

4 Yang Liu ^{†,‡,*}, Jan Baas ^{‡,§}, Willie J.G.M. Peijnenburg ^{‡,||}, Martina G. Vijver [‡]

5

6 [†] Faculty of Environmental Science and Engineering, Kunming University of Science and
7 Technology, 650500 Kunming, Yunnan Province, China

8 [‡] Institute of Environmental Sciences (CML), Leiden University, 2300 RA Leiden, The
9 Netherlands

10 [§] Centre for Ecology & Hydrology (CEH), MacLean Building, Benson Lane, OX10 8BB
11 Wallingford, Oxfordshire, United Kingdom

12 ^{||} National Institute of Public Health and the Environment (RIVM), Center for Safety of
13 Substances and Products, 3720 BA Bilthoven, The Netherlands

14

15 * Corresponding author. Tel.: +31(0)71 527 7477; fax: +31 (0)71 527 7434; e-mail address:
16 minipig6@163.com (Yang Liu)

17 Text words excluding references: 5359

18 Small tables: 3 (900 words)

19 Small figures: 2 (600 words); Large figures: 1 (600 words)

20 Supporting information: 3 figures and 2 tables

21 Total words: 7459

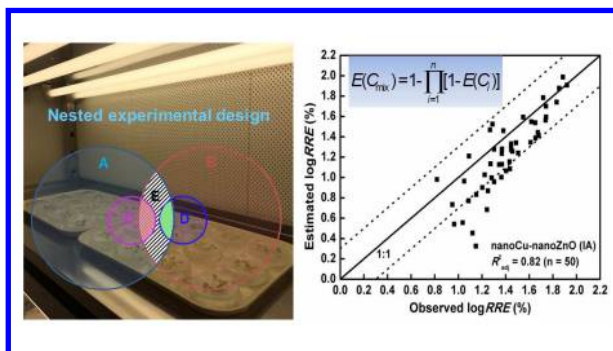
22 **Abstract**

23 Little is understood regarding the effects of mixtures of different metal-based nanoparticles
24 (NPs). Using concentration addition (CA) and independent action (IA) models, we evaluated
25 the combined toxicity of Cu and ZnO NPs based on five nested combinations, i.e. Cu(NO₃)₂-
26 CuNPs, Zn(NO₃)₂-ZnONPs, Cu(NO₃)₂-ZnONPs, Zn(NO₃)₂-CuNPs, and CuNPs-ZnONPs on
27 root elongation of *Lactuca sativa* L. The CA and IA models performed equally well in
28 estimating the toxicity of mixtures of Cu(NO₃)₂-CuNPs, Zn(NO₃)₂-ZnONPs and Zn(NO₃)₂-
29 CuNPs, whereas the IA model was significantly better to fit the data of Cu(NO₃)₂-ZnONPs
30 and CuNPs-ZnONPs mixtures. Dissolved Cu proved to be the most toxic metal species to
31 lettuce roots in the tests, followed by Cu NPs, dissolved Zn, and ZnO NPs respectively. An
32 antagonistic effect was observed for ZnO NPs on the toxicity of Cu NPs. This antagonistic
33 effect is expected to be the result of interactions between dissolved Cu and dissolved Zn,
34 particulate Zn and dissolved Zn, particulate Cu and dissolved Zn, and between particulate
35 Zn and dissolved Cu. In general terms, assuming additivity gives a first indication of the
36 combined toxicity with soluble and insoluble metal particles both being important in driving
37 toxicity of metal-based NPs to higher plants.

38 **Keywords:** Cu, Zn, nanoparticles, mixture, toxicity

39

40 Abstract graphic image



41

42

43

44

45

46

47

48

49

50

51

52

53

54

55

56 1. Introduction

57 Nanotechnology has been applied to create novel materials with unique characteristics in a
58 large variety of consumer and household products. For example, engineered zinc oxide
59 nanoparticles (NPs) are added into personal care products and coatings, which benefit from
60 their ability to efficiently absorb UV-light and their increased transparency to visible light¹.
61 Nano-Cu powders can be dispersed into catalysts, conductive pastes, sintering additives,
62 anti-bacteria products, and lubricant additives owing to their potential catalytic, dielectric, and
63 biomedical properties².

64 Dissolution and aggregation/agglomeration are the two main processes that can strongly
65 influence the state of metal-based NPs present in suspensions, and consequently impact the
66 bioavailability, uptake and toxicity of NPs³. It has been reported that various characteristics
67 of the exposure media can affect dissolution and aggregation of metal-based NPs, e.g. pH,
68 ionic strength and the presence of naturally occurring organic matter⁴. Dissolution of NPs is
69 a dynamic process in which constituent molecules of the dissolving solid migrate from the
70 surface to the bulk solution through a diffusion layer⁵. The adsorption of molecules and ions
71 from solution can promote or delay the dissolution process by modifying the characteristics
72 of the diffusion layer⁶. Apart from heteroaggregation, particles can also be bound together
73 (homoaggregation) when their equilibrium solubility is above saturation concentrations⁷,
74 which can increase the overall diffusion layer thickness and hinder dissolution of NPs.

75 Increasing numbers of applications may lead to direct or indirect releases of engineered
76 metal-based NPs into the environment. This may pose effects on a variety of organisms in
77 aquatic and terrestrial ecosystems, and in turn requires more attention on their eco-
78 toxicological effects. Metal-based NPs are commonly predicted to occur in the environment
79 as colloids⁸. Metal ions or small inorganic complexes produced by engineered metal-based
80 NPs consisting of highly toxic elements inevitably drive the partial toxicity of metal-based
81 NPs to organisms³. However, it is still a challenge to clarify which metal species contribute
82 most to the nano-toxicity. Some studies suggested that the toxic effects of ZnO NPs and Cu

83 NPs on organisms were most likely due to the dissolved metal species rather than being
84 particle-dependent⁹⁻¹¹. Other researchers argued that the particulate forms of ZnO NPs and
85 Cu NPs contributed substantially to the cytotoxic effects on mammalian and piscine cell lines
86^{12, 13}. The translation from an effect on a cell line to a whole organism is not straightforward
87 and depends on numerous factors such as the type of cell lines used and the physical and
88 chemical composition of the NPs under consideration. Karlsson et al.¹⁴ found for instance
89 that the oxidative stress of mouse embryonic stem (mEs) cells was induced by the released
90 Cu ions of CuO NPs whereas the stress was particle related for NiO NPs.

91 The lowest median L(E)C₅₀ value for nano-ZnO to aquatic organisms was observed to be
92 <0.1 mg/L. This value classifies nano-ZnO as being 'extremely toxic', whereas the lowest
93 values of L(E)C₅₀ (0.1~1 mg/L) classify nano-Cu as 'very toxic'¹⁵. These NPs were found to
94 be simultaneously present in wastewater effluents¹⁶⁻¹⁸. They thus can jointly enter the
95 terrestrial system by the application of bio-solids from sewage systems as a fertilizer¹⁹.
96 Plants such as *Lactuca sativa* and *Medicago sativa*²⁰ have been reported to be able to take
97 up and store metal-based NPs in their tissues²¹. To date, the knowledge of the eco-toxicity
98 of Cu NPs and ZnO NPs is far from being adequate as compared to their large-scale
99 application^{22, 23}, especially under conditions of co-exposure.

100 This study aims at improving the understanding of the effects of Cu NPs, ZnO NPs and their
101 mixtures on *L. sativa* L. by unravelling the following two research questions: (1) Will the
102 dissolved metals and the particulate metals of each type of metal-based NPs act jointly
103 following the common rules of additivity? (2) Will Cu NPs interact with ZnO NPs and
104 influence the toxicity of each other? Theoretically, if Cu NPs and ZnO NPs would act
105 comparable to their metal salts, the existing models for predicting the combined effects of
106 metals can be applied to predict the toxicity of mixtures of metal-based NPs. As shown in our
107 previous studies^{24, 25}, Cu²⁺ competed with Zn²⁺ for binding to the biotic ligand of lettuce.
108 However, this research is more complex than in case of mixtures of metal salts because
109 suspensions of each type of metal-based NPs consist of a mixture mainly containing

110 dissolved metal species and undissolved particles. Suspensions of Cu NPs and ZnO NPs
111 will therefore contain four metal species that are relevant to the toxicity of mixtures, i.e.
112 dissolved Cu, dissolved Zn, particulate Cu and particulate ZnO. Cedergreen et al.²⁶ have
113 shown that the joint effect of ternary mixtures can be predicted from binary mixture toxicity
114 results. Thus, an elaborate nested experiment (binary, ternary, quaternary mixtures) was
115 designed to include all possible combinations in order to trace down the potential
116 'interactions' between Cu NPs and ZnO NPs and where these 'interactions' (if any) take
117 place. The two classic concepts of additivity i.e. concentration addition (CA) and
118 independent action (IA) were both used for mixture toxicity predictions. A $\text{Zn}(\text{NO}_3)_2$ or
119 $\text{Cu}(\text{NO}_3)_2$ solution was applied as a reference to assess the behavior of the dissolved Zn or
120 Cu from the NPs in solution. The combined effects on root growth by nanoCu-nanoZnO
121 mixtures were then compared with the overall effects of $\text{Cu}(\text{NO}_3)_2$ and $\text{Zn}(\text{NO}_3)_2$ reported in
122 previous studies. The following combinations were studied:

- 123 • $\text{Cu}(\text{NO}_3)_2$ and Cu NPs (dissolved Cu and particulate Cu, Cu-nanoCu)
- 124 • $\text{Zn}(\text{NO}_3)_2$ and ZnO NPs (dissolved Zn and particulate ZnO, Zn-nanoZnO)
- 125 • $\text{Zn}(\text{NO}_3)_2$ and Cu NPs (dissolved Zn, dissolved Cu and particulate Cu, Zn-nanoCu)
- 126 • $\text{Cu}(\text{NO}_3)_2$ and ZnO NPs (dissolved Cu, dissolved Zn and particulate ZnO, Cu-nanoZnO)
- 127 • Cu NPs and ZnO NPs (dissolved Cu, dissolved Zn, particulate Cu and particulate ZnO,
128 nanoCu-nanoZnO)

129 **2. Methods**

130 **2.1 Test compounds and nutrient solution**

131 Uncoated Cu NPs (nano-spheres, nominal particle size 50 nm, coded NM-0014, purity
132 99.8%) and uncoated ZnO NPs (nano-sticks, nominal particle size 150 nm, coded NM-110)
133 were purchased from the io-li-tec company (Heilbronn, Germany). $\text{Cu}(\text{NO}_3)_2 \cdot 3\text{H}_2\text{O}$ (purity
134 99.5%), $\text{Zn}(\text{NO}_3)_2 \cdot 6\text{H}_2\text{O}$ (purity 99.5%) and other salts used in preparing the nutrient solution
135 were all purchased from the Merck KGaA company (Darmstadt, Germany). The nutrient

136 solution was composed of $\text{Ca}(\text{NO}_3)_2 \cdot 4\text{H}_2\text{O}$ (236.1 mg/L), $\text{MgSO}_4 \cdot 7\text{H}_2\text{O}$ (60 mg/L), NaHCO_3
137 (50 mg/L), and KHCO_3 (10 mg/L) totally dissolved in demi-water (pH 7.8) and was applied
138 for culturing plants and preparing the exposure media.

139 **2.2 Experimental design**

140 To allow the data to be interpreted over a wide range of concentrations of particulate and
141 dissolved species of Cu and Zn, the composition of the five mixtures was chosen according
142 to a full factorial experimental design. The nominal concentrations of $\text{Cu}(\text{NO}_3)_2$ ranged from
143 0.06 to 0.30 mg/L, the range of $\text{Zn}(\text{NO}_3)_2$ was from 2.90 to 17.39 mg/L, the range of Cu NPs
144 was from 0.10 to 0.80 mg/L, and the range of ZnO NPs was from 0.50 to 50.00 mg/L. A
145 detailed description of the experimental setup after pre-screening tests is provided in Table
146 S1 on the basis of actual concentrations. Mixture treatments of each combination were
147 repeated twice with negative controls (nutrient solution) and positive controls (single
148 compounds, i.e. $\text{Cu}(\text{NO}_3)_2$, $\text{Zn}(\text{NO}_3)_2$, Cu NPs, ZnO NPs individually) for further analysis
149 (section 2.6) and to reduce the variation of non-simultaneous toxicity tests. Hydroponic
150 exposure was used as a starting point to study the mutual impacts between metal-based
151 NPs and to avoid interference from complex interactions with soil particles. To keep the
152 concentrations of compounds in solution constant, the test media were replaced every day.
153 Stock suspensions of Cu NPs and ZnO NPs were daily prepared in nutrient solution and
154 sonicated in an S 40 H Elmasonic water bath sonicator (Elma, Germany) for 10 min. All the
155 stock solutions including the nitrate salts were further diluted 10 times with nutrient solution
156 to obtain the nominal concentrations for each treatment.

157 **2.3 Exposure of lettuce and toxicity determination**

158 *Lactuca sativa* L. was selected as the test organism because its bioassay has been
159 recommended to be a relatively easy and quick way of evaluating potential environmental
160 risks by the Organization for Economic Cooperation and Development (OECD)²⁷. The
161 toxicity tests were performed according to guidelines of the US Environmental Protection
162 Agency (EPA)²⁸. As compared to the germination rate of seeds, the relative root elongation

163 rate (*RRE*, %) of lettuce seedlings is more accurate and more effective in reflecting the
164 impact of external stressors²⁹, and therefore *RRE* was exploited as the toxicological
165 endpoint in this study. Lettuce seeds were purchased from the Horti Tops company
166 (Amsterdam, the Netherlands) and germinated on expanded perlite in a climate room (18°C,
167 80% humidity, and a 16:8 h light: dark cycle) for 96 h. After germination, seedlings with
168 taproot lengths more than 3 cm were chosen to be fixed on parafilm strips floating on the
169 surface of glass petri dishes containing 30 ml test medium. In each petri dish, 4 seedlings
170 were introduced. Before and after 96 h exposure, the length of lettuce taproot was measured
171 from the transition point between the hypocotyls and the root to the root tip. The root growth
172 of each treatment was defined as the mean value of differences in root length of 4 seedlings
173 before and after exposure. Then *RRE* was determined according to equation 1:

174
$$RRE = \frac{RG_s}{RG_c} \times 100\% \quad (1)$$

175 RG_s : the root growth of plants in the sample solution, cm;

176 RG_c : the root growth of plants in the control solution, cm.

177 **2.4 Characterization of nanoparticles**

178 The primary morphology and particle size of metal-based NPs prepared in lettuce culture
179 medium were characterized using a JEOL 1010 Transmission Electron Microscope (TEM,
180 JEOL, Japan). The particle size of Cu NPs and ZnO NPs was analyzed using a Nano
181 Measurer 1.2 (Fudan University, China). The distribution of hydrodynamic diameter and the
182 zeta-potential of NPs in seven types of test media (i.e. nano-Cu, nano-ZnO, Cu-nanoCu, Zn-
183 nanoZnO, Cu-nanoZnO, Zn-nanoCu, nanoCu-nanoZnO mixtures prepared in lettuce culture
184 medium) were measured after 1 h and 24 h of preparation by Dynamic Light Scattering (DLS)
185 on a Zetasizer Nano-ZS instrument (Malvern, United Kingdom).

186 **2.5 Chemical analysis**

187 A Cu-ion selective electrode (Cu-ISE, Metrohm, Switzerland) was used as a direct way to
188 measure the free Cu-ion activity in solution after 1 h and 24 h. A Zn-ion selective electrode

189 was not used in this study because the detection limit was not sufficient for the test. To
190 check whether particles will reduce the sensitivity of the Cu-electrode membrane, plain
191 polystyrene fluorescent microspheres # 103125-05 (nominal particle size 70 nm,
192 Microspheres-Nanospheres, American) were added to compare the activities of Cu^{2+} with
193 those in solutions of $\text{Cu}(\text{NO}_3)_2$ alone. The actual total concentrations of Ca, Mg, Na, K, Cu,
194 Zn, and the dissolved concentrations of Cu and ZnO NPs after 1 h and 24 h of equilibration
195 were analyzed using Flame Atomic Absorption Spectroscopy (FAAS, Perkin Elmer AAnalyst
196 100, American). Centrifugation of samples removed particles from suspensions. The
197 supernatants were obtained and used for testing after 20 min of centrifugation in a
198 Centrifuge 5415D (Eppendorf, Germany) at $13\,300\text{ g}^{12}$. The particle suspensions, the
199 supernatants and the liquids with nitrate salts were digested using HNO_3 and sampled for
200 FAAS analysis.

201 **2.6 Data analysis**

202 To check the potential chemical-chemical interactions before entering the organism,
203 relationships between the free Cu^{2+} activities in the solution (or the dissolved metal species
204 of Cu NPs or ZnO NPs) and the added amount of one compound in mixtures of Cu-nanoCu,
205 Zn-nanoZnO, Cu-nanoZnO, Zn-nanoCu, and nanoCu-nanoZnO after 1 h and 24 h were all
206 analyzed using the linear regression method in the GraphPad Prism 5 software (GraphPad,
207 American). For the Cu-nanoCu mixtures, the activities of Cu^{2+} released from Cu NPs were
208 calculated by subtracting the Cu^{2+} activities of $\text{Cu}(\text{NO}_3)_2$ from the totally measured activities
209 of Cu^{2+} in mixture solutions. The actually total or dissolved concentrations of Cu NPs or ZnO
210 NPs in Cu-nanoCu and Zn-nanoZnO mixtures were calculated in a similar way.

211 The independent action (IA) model and the concentration addition (CA) model based on the
212 rules of 'additivity'³⁰ were both used to predict the combined toxicity of mixtures of Cu-
213 nanoCu, Zn-nanoZnO, Cu-nanoZnO, Zn-nanoCu and nanoCu-nanoZnO. The observed
214 effects were then compared with the estimated values of CA or IA models. By definition, the
215 basic assumption of additivity is that one compound is non-interactive with the other

216 compounds in a mixture³¹. The CA model is thought to be valid for mixtures where the
 217 components have similar target sites and a similar mode of action (MoA)³². The concept of
 218 IA originates from statistical considerations of independent responses and is supposed to be
 219 satisfactory for modeling effects of mixtures where the components differ in uptake pathways
 220 or MoA³⁰. However, information on detailed MoA is still not available for the majority of
 221 chemicals³³. Thus, the additive effects of mixtures were predicted by both multiplying the
 222 responses of mixture components (for IA), and by summing the scaled exposure levels (for
 223 CA) in this study. The IA model is mathematically presented by equation 2:

$$224 \quad E(C_{\text{mix}}) = 1 - \prod_{i=1}^n [1 - E(C_i)] \quad (2)$$

225 $E(C_{\text{mix}})$: the estimated effect of an n-compound mixture;

226 $E(C_i)$: the effect of the i th compound applied singly at a fixed concentration, relative to the

227 RGc of untreated controls.

228 To facilitate the estimation of toxic effects of mixtures on the basis of concentration addition,
 229 the sum of toxic units (TU_{mix} , a dimensionless ratio) was introduced to represent the toxic
 230 strength of a mixture³⁴. Strict concentration addition occurs when the value of TU_{mix} equals
 231 one according to equation 3:

$$232 \quad TU_{\text{mix}} = \sum_{i=1}^n \frac{c_i}{EC_{xi}} \quad (3)$$

233 c_i : the concentration of individual compound i in the mixture with n compounds;

234 EC_{xi} : the effect concentration of individual compound i that results in the same effect (x%)

235 as the mixture. The concentration-response relationship of a mixture was obtained using the

236 logistic function³⁵ presented in equation 4 programmed in OriginPro 8 (Origin Lab, United

237 Kingdom):

$$238 \quad RRE = \frac{100}{1 + \left(\frac{TU_{\text{mix}}}{TU_{\text{mix}}^{50\%}}\right)^\beta} \quad (4)$$

239 *RRE*: RG_s of mixture treatments relative to RG_c of negative controls; β the shape parameter
240 that determines the steepness of the response curves; $TU_{mix}^{50\%}$: the sum of toxic units of a
241 mixture inducing 50% inhibition of root elongation.

242 If compounds in a mixture do not follow the rules of 'additivity', 'interactions' between
243 compounds may either increase or decrease the toxicity of mixtures relative to the model
244 predictions³⁶. Finding interactions in mixtures is always a challenge, especially when a
245 mixture contains more than two components. Since the suspensions of mixtures of Cu-
246 nanoZnO, Zn-nanoCu, and nanoCu-nanoZnO contain more than two metal species,
247 searching interactions between these different metal species cannot be done using the
248 existing models for binary mixtures. Therefore, a different approach was used in this study,
249 which will be explained by the following example of Cu-nanoZnO mixtures.

250 To examine the influence of $Cu(NO_3)_2$ on the toxicity of ZnO NPs, the median effective
251 concentrations (EC_{50}) of ZnO NPs in the co-exposure with $Cu(NO_3)_2$ were compared with the
252 EC_{50} value of ZnO NPs in single exposure. The *RREs* induced by ZnO NPs in co-exposure
253 with $Cu(NO_3)_2$ can be calculated using the root growth of positive controls (with $Cu(NO_3)_2$
254 alone) as RG_c in equation (1). The *RREs* induced by ZnO NPs alone can be calculated by
255 using the root growth of negative controls (nutrient solution only) as RG_c in equation (1). The
256 EC_{50} s of ZnO NPs in single-exposure or co-exposure with $Cu(NO_3)_2$ were calculated using
257 the log (inhibitor) vs. normalized response-variable slope function in GraphPad Prism 5. It
258 was assumed that if the EC_{50} s of ZnO NPs in the co-exposure with $Cu(NO_3)_2$ were
259 significantly different from the value of ZnO NPs in single exposure, then the influence of
260 $Cu(NO_3)_2$ on the toxicity of ZnO NPs was statistically significant. The EC_{50} values of ZnO NPs
261 were plotted as a function of increasing concentrations of $Cu(NO_3)_2$ following linear
262 regression in OriginPro 8. As an initial attempt, the slope of the obtained straight lines was
263 compared with zero to indicate the overall antagonism or synergism. A non-significant slope
264 is indicative of no substantial interactive effects of $Cu(NO_3)_2$ on the toxicity of ZnO NPs, a

265 significant positive ($p < 0.05$) slope implies the decreased toxicity of ZnO NPs by $\text{Cu}(\text{NO}_3)_2$
266 or the occurrence of antagonistic effects of $\text{Cu}(\text{NO}_3)_2$ on ZnO NPs, and a significant negative
267 slope indicates the increased toxicity of ZnO NPs by $\text{Cu}(\text{NO}_3)_2$ or synergistic effects. Similar
268 methods can be used to find out the influence of ZnO NPs (in both dissolved and particulate
269 forms) on the toxicity of $\text{Cu}(\text{NO}_3)_2$ and for other mixtures investigated in this study.

270 **3. Results**

271 **3.1 Characterization of nanoparticles**

272 The TEM images of Cu NPs, ZnO NPs and their mixtures are shown in Figure 1. The
273 primary sizes and shapes of the particles were estimated based on the TEM images. The Cu
274 NPs were shown to be of spherical shape, 127 nm in size (size variation of 119-137 nm).
275 The ZnO NPs crystals displayed an approximatively tetragonal morphology (width: 55 nm,
276 size variation of 24-110 nm; length: 144 nm, size variation of 95-224 nm). The size
277 distribution of the hydrodynamic diameter of NPs in lettuce culture solution and in
278 suspensions of the five combinations investigated was determined using DLS and are shown
279 in Table S2. Initial particle sizes changed quickly after the NPs were submerged in lettuce
280 culture solution. Both NPs were present as aggregates (370 nm - 1531 nm) in lettuce culture
281 solution and in mixture suspensions. The hydrodynamic particle sizes of Cu NPs and ZnO
282 NPs increased by a factor of 1.5 to 2 after being submerged for 24 h in lettuce culture
283 solution and in suspensions of mixtures of Zn-nanoCu, nanoCu-nanoZnO, Zn-nanoZnO.

284 **3.2 Fate analysis**

285 Relationships between the free activities of Cu^{2+} in solution and added ZnO NPs, $\text{Zn}(\text{NO}_3)_2$,
286 Cu NPs, $\text{Cu}(\text{NO}_3)_2$ after 1 h and 24 h are plotted in Figure S1. After 24 h, the activities of
287 Cu^{2+} were generally increased in mixtures of Cu-nanoCu, Zn-nanoCu, Cu-nanoZnO, and
288 nanoCu-nanoZnO as compared to the values after 1 h. However, no consistently significant
289 effects of increasing concentrations of $\text{Cu}(\text{NO}_3)_2$, Cu NPs, $\text{Zn}(\text{NO}_3)_2$, ZnO NPs were
290 observed on the activities of Cu^{2+} in solution after 1h and 24 h of equilibration using the Cu-

291 ISE. This indicated that the amount of free Cu^{2+} released from either Cu NPs or $\text{Cu}(\text{NO}_3)_2$
292 was not substantially affected by other compounds of Cu or Zn added to the solution. It is
293 shown in Figure S2 that the trend of increasing Cu^{2+} activities in solution with polystyrene
294 fluorescent microspheres remained constant when more $\text{Cu}(\text{NO}_3)_2$ was added and the slope
295 of linear curves remained positive.

296 The background concentrations of Na, K, Ca, Mg in nutrient solution were measured to be
297 respectively 11.9 ± 0.3 mg/L, 3.68 ± 0.07 mg/L, 31.24 ± 0.5 mg/L, and 5.49 ± 0.08 mg/L. The
298 impacts of other compounds on the dissolved concentrations of Cu NPs and ZnO NPs after
299 1h and 24 h of equilibration in mixtures of Cu-nanoCu, Zn-nanoZnO, Cu-nanoZnO, Zn-
300 nanoCu, nanoCu-nanoZnO are represented in Figure S3. Generally, the more NPs were
301 added to the solution, the lower the percentage of dissolved metal-based NPs was
302 measured after 1 h and 24 h. The dissolved concentrations of Cu NPs at the same
303 concentration levels were found to be higher after 24 h in all combinations, which coincided
304 with increases of the free Cu^{2+} activities. No statistically significant and consistent impacts
305 were observed from addition of $\text{Zn}(\text{NO}_3)_2$, $\text{Cu}(\text{NO}_3)_2$, and Cu NPs on the dissolution of ZnO
306 NPs. Although the dissolved concentrations of Cu NPs at lower concentrations were
307 significantly increased by the added $\text{Cu}(\text{NO}_3)_2$ after 1 h, the influence was not constant
308 across the whole range of concentrations. Only for Zn-nanoCu mixtures, it was found that
309 after 24 h the dissolved concentrations of Cu NPs were significantly reduced by the addition
310 of $\text{Zn}(\text{NO}_3)_2$.

311 **3.3 Toxicity of individual compounds**

312 Following the full factorial experimental design, a complete concentration-response curve
313 was obtained for each compound investigated in this study, which was used to calculate the
314 EC_{50} to *L. sativa* L. As shown in Table 1, ZnO NPs had the lowest acute toxicity to lettuce
315 roots. By contrast, $\text{Cu}(\text{NO}_3)_2$ showed the highest toxic effects on root growth, which was
316 followed by Cu NPs and $\text{Zn}(\text{NO}_3)_2$. The EC_{50} values of Cu NPs and $\text{Cu}(\text{NO}_3)_2$ were similar,
317 but the EC_{50} value of ZnO NPs was twice as high as for $\text{Zn}(\text{NO}_3)_2$.

318 **3.4 Toxicity of mixtures**

319 The accuracy of model predictions is shown in Figure 2 and Table 2. Generally, 62%~100%
320 of the estimated values of *RRE* were within a factor of 2 of the observed values. On the
321 basis of 'additivity' or no interactions, the IA model performed better than the CA model in
322 estimating toxicity of Cu-nanoCu, Zn-nanoZnO, Cu-nanoZnO, and nanoCu-nanoZnO
323 mixtures at different exposure levels, as evidenced by a 0.04~24 percentage of increase in
324 R^2 . Apart from the combination of Cu-nanoCu, the combined effects of Zn-nanoZnO, Zn-
325 nanoCu, Cu-nanoZnO, and nanoCu-nanoZnO mixtures were mostly underestimated using
326 the IA model (Figure 2 F-J). This indicated that the predictive ability of IA and CA models
327 was also combination-specific for mixtures with metal-based NPs.

328 To examine whether 'interactions' were the cause of remaining deviations from the model,
329 the effective concentrations causing a 50% reduction in root elongation of Cu NPs, ZnO NPs,
330 $\text{Cu}(\text{NO}_3)_2$, $\text{Zn}(\text{NO}_3)_2$ in single-exposure and in co-exposures of Cu-nanoCu, Zn-nanoZnO,
331 Cu-nanoZnO, Zn-nanoCu, and nanoCu-nanoZnO were plotted as a function of various
332 concentration levels of Cu or Zn in solution (Figure 3). Significant linear fits ($p < 0.05$) with a
333 positive slope were generally found in four out of five combinations, which indicated overall
334 antagonistic effects between mixture components. In Figure 3 A-D, the EC_{50} values of nano-
335 Cu were shown not to be statistically significantly increased upon increasing concentrations
336 of $\text{Cu}(\text{NO}_3)_2$ and significant impacts of Cu NPs on the EC_{50} s of $\text{Cu}(\text{NO}_3)_2$ were neither
337 observed. This implied that the dissolved Cu and the particulate Cu did not affect the toxicity
338 of each other to lettuce (Table 3). For the combination of Cu-nanoZnO, the EC_{50} values of
339 nano-Zn and $\text{Cu}(\text{NO}_3)_2$ cannot be accurately calculated when concentrations were beyond
340 40 mg/L and 0.06 mg/L respectively due to the small difference in root length as compared
341 to positive controls. Without these data points, the EC_{50} values of $\text{Cu}(\text{NO}_3)_2$ were significantly
342 increased upon increasing amounts of ZnO NPs in the solution (F-H, Figure 3), and the
343 EC_{50} s of nano-Zn were significantly increased, up to a factor of 5.5 at 0.05 mg/L of $\text{Cu}(\text{NO}_3)_2$
344 (small graph inside E, Figure 3). For the combination of Zn-nanoCu, the EC_{50} s of $\text{Zn}(\text{NO}_3)_2$

345 were found to be sharply increased by the added Cu regardless of the metal species in
346 solution, and a similar result was observed in turn at low concentrations (small graph inside I,
347 Figure 3). The EC_{50} values of nano-ZnO significantly increased upon increasing
348 concentrations of $Zn(NO_3)_2$ in solution. At lower concentrations of ZnO NPs, the EC_{50} s of
349 $Zn(NO_3)_2$ were also increased with increasing concentrations of Zn NPs (small graphs inside
350 N-P, Figure 3). This finding indicated that the dissolved Zn may compete against the
351 particulate Zn for inducing toxicity to lettuce at lower concentrations of Zn NPs (< 20 mg/L).
352 For nanoCu-nanoZnO mixtures, without the EC_{50} s of ZnO NPs at higher concentrations of
353 Cu NPs, non-significant impacts of Cu NPs (<0.05 mg/L) were observed on the toxicity of
354 ZnO NPs. The EC_{50} s of Cu NPs were observed to be significantly increased with an
355 increased amount of ZnO NPs in solution (< 5mg/L).

356 **4. Discussion**

357 ***4.1 Fate of nanoparticles***

358 The absolute values of the zeta-potential were < 14 mV, which implied that suspensions of
359 NPs were unstable and general aggregation of the particles was observed because of the
360 Van Der Waals inter-particle forces. This explained why the hydrodynamic size of Cu NPs
361 and ZnO NPs in culture media of lettuce was not observed to be strongly affected by
362 addition of $Cu(NO_3)_2$ and $Zn(NO_3)_2$ after 1 h and 24 h of equilibration. The high
363 concentrations of salts in the nutrient solution can be an additional reason for the rapid
364 aggregation observed⁴. The dissolution or ion release of Cu NPs or ZnO NPs was
365 insignificantly and inconsistently hindered or stimulated by the increasing concentrations of
366 Cu or Zn in the exposure media except in Zn-nanoCu mixtures after 24 h. The observation of
367 significant impacts of Zn on the dissolution of Cu NPs may be related to the $Zn(NO_3)_2$
368 concentrations used which were in between 3.23 and 100 times higher than the
369 concentrations of Cu NPs. The increasing amount of Zn^{2+} in water may bind to the negatively
370 charged surface of Cu NPs, and thus hinder the dissolution of Cu NPs by increasing
371 thickness of the diffusion layer of NPs or by introducing kinetic hindrance to the Cu^{2+}

372 diffusion process⁵. Nevertheless, a similar observation was not made for nanoCu-nanoZnO
373 mixtures, which implied that the impacts of nanoZnO on dissolution of nanoCu were not
374 concentration-dependent only. Alternatively, unlike the other properties of water chemistry
375 such as pH, HPO_4^{2-} and DOM³⁷, the increased background concentrations of Cu and Zn
376 may not strongly influence the dissolution of Cu NPs and ZnO NPs. Further research is still
377 needed on how to accurately quantify these two competing processes (i.e. dissolution and
378 aggregation) and their mutual impacts in water system for metal-based NPs.

379 **4.2 Toxicity of individual compounds**

380 In this study, we found that both Cu NPs and ZnO NPs reduced the root size of lettuce.
381 Although copper and zinc are essential for plant growth, they are also toxic to plants at
382 concentrations that exceed critical levels³⁸. The decrease of nutrients such as P and Fe, the
383 alteration of enzyme activity²⁰, and the higher production of reactive oxygen species (ROS)³⁹
384 within the plants may be explanations for the impacts of metal-based NPs on lettuce growth.
385 In addition, the portion of aqueous Cu species dissolved from Cu NPs may also damage the
386 plasmalemma of root cells and result in loss of K, N, and other solutes⁴⁰. Results of the
387 present study and of the previous studies showed that Cu is more toxic to lettuce seedlings
388 than Zn regardless of the metal being in the form of a cation or nanoparticles. This suggests
389 metal-specific responses of lettuce or different toxicokinetics of excess Cu and Zn in
390 terrestrial plants. However, the EC_{50} of dissolved Zn calculated in this study was significantly
391 lower than the value predicted for Zn^{2+} in the research of Le et al.²⁴. This difference can be
392 the result of differences in the chemical composition of the background medium used and
393 the subsequent variation in speciation as calculated by the Windermere Humic-Aqueous
394 Model VI. Additionally, the effects of Cu or Zn seemed to be associated with the form of the
395 metal species that the relatively lower EC_{50} values of nitrate salts were calculated in this
396 study as compared to the corresponding nanoparticles. This finding was consistent with the
397 research of Hong et al.²⁰, in which the size of particles was shown to play an important role
398 in Cu uptake.

399 **4.3 Combined toxicity of Cu NPs and ZnO NPs**

400 **4.3.1 Comparison of CA and IA models**

401 The present study used the CA as well as the IA model to assess the combined toxicity of
402 mixtures and their departures from additivity. The CA concept is usually proposed as a
403 default conservative option as compared to the IA concept, which was also the case in our
404 study. However, the fitting performance of the IA model was significantly better than the
405 fitting performance of the CA model based on the value of R^2 for combinations of Cu-
406 nanoZnO and nanoCu-nanoZnO. This is different from the findings of our previous studies^{41,}
407⁴² showing that the combined effects of binary metal mixtures with Cu were equally well
408 explained by these two classic mixture models. The mechanisms of toxicity of metal-based
409 NPs in co-exposure were so complex that they cannot be directly extrapolated from normal
410 metal mixtures. Therefore, it is suggested that both models should remain as statistical
411 statements of joint effects, especially for mixtures of metal-based NPs.

412 **4.3.2 Comparison with previous research**

413 The good fittings provided by IA and CA ($R^2_{adj}=0.90\sim0.94$) models and the non-significant
414 'interactions' observed between dissolved and particulate Cu simultaneously verified the
415 assumption of Song et al.¹³ that addition models can be used to estimate the relative
416 contributions of ionic and particulate forms to the cytotoxicity of Cu NPs. Both models also
417 showed reasonable predictive power in estimating toxicity of Zn-nanoZnO mixtures
418 ($R^2_{adj}=0.79\sim0.83$). Antagonistic interactions were identified between dissolved and
419 particulate Zn which helped explain variations in modelling. Antagonistic effects were also
420 observed for dissolved Zn or Cu resulting from NPs on the toxicity of their nitrate salts
421 (Figure 3 G, K). This was consistent with the competition between Cu^{2+} and Zn^{2+} at the
422 organism level reported in previous studies^{24, 25, 36}. The feed-back mechanism⁴³ explained
423 that an increase of copper in plant cell decreases the quantity of zinc importer proteins and
424 blocks channels for zinc. In turn, the presence of low amounts of zinc may exert a positive
425 effect on cell homeostasis and on the tolerance of cells to copper¹⁸. Until now, only Li et al.

426 ¹⁸ reported (1) the potentiation effects on the human hepatoma cell line HepG2 co-exposed
427 to Cu NPs and ZnO NPs and (2) suggested that the nano-particulate ZnO NPs were
428 attributable to the enhancement of Cu NPs toxicity. By contrast, ZnO NPs were observed to
429 have an antagonistic effect on the impact of Cu NPs on root growth of lettuce at low
430 concentrations, whereas the toxicity of ZnO NPs was insignificantly affected by Cu NPs. This
431 difference may be caused by different features between animal cells and plant cells which
432 lead to a diverse bioavailability or toxicity across species. Additionally, the one-sided
433 antagonistic effects may be because the Zn concentrations were many times higher than the
434 concentrations of Cu in the mixtures³⁶. In compliance with the second finding of Li et al.¹⁸,
435 the particulate NPs were also observed to correlate with the 'interactions' and the overall
436 toxicity of Cu NPs and ZnO NPs, which may be due to their physical effects⁸ produced on
437 the plant surface.

438 In summary, the concentration addition and independent action models performed equally
439 well in assessing the combined toxicity of Cu-nanoCu, Zn-nanoZnO, and Zn-nanoCu
440 mixtures on lettuce roots. However, for the combinations of Cu-nanoZnO and nanoCu-
441 nanoZnO, the IA model significantly accounted for more variation in root growth. Based on
442 the results of the Cu-nanoCu, Zn-nanoZnO, Zn-nanoCu, Cu-nanoZnO mixtures, the one-
443 sided antagonistic effects observed for nanoCu-nanoZnO mixtures may be attributed to
444 'interactions' occurring between dissolved Cu and dissolved Zn, particulate Zn and dissolved
445 Zn, particulate Cu and dissolved Zn, particulate Zn and dissolved Cu. It was thus
446 demonstrated that considering various species of Cu NPs and ZnO NPs in water (dissolved
447 and particulate) is of great importance for assessing their toxicity to terrestrial plants. The
448 combined effects of dissolved species from NPs were similar to the effects produced by
449 common metal mixtures. To our knowledge, exposure methods have been mostly used for
450 assessing the ecological effects of single type NPs. Considering naturally occurring
451 conditions, our experiments constitute the first study of mixture effects of NPs to higher
452 plants. Although detailed information of interactive mechanisms of metal-based NPs with

453 their environment remains to be obtained, there is no doubt that this research will enrich the
454 rapid evolving field of nano-toxicology and help scientists develop approaches to evaluate
455 the potential impacts of metal-based NPs and their mixtures on ecosystems.

456 **Acknowledgments**

457 Supports provided to MG Vijver by the NWO VIDI project (No. 864.13.010), to J Baas by the
458 EU Marie Curie BIOME project (No. 328931), and to WJGM Peijnenburg by the EU-
459 sponsored FP7 project 'FutureNanoNeeds' (No. 604602) are gratefully acknowledged. The
460 authors thank Marcel Biermans for assisting in experiments.

461 **Declaration of interest**

462 The authors declare no competing financial interest.

463 **Supporting Information.** Figure S1 of relationships between free Cu^{2+} activities and the
464 added amount of ZnO NPs, $\text{Zn}(\text{NO}_3)_2$, Cu NPs, $\text{Cu}(\text{NO}_3)_2$, Figure S2 of relationships
465 between free Cu^{2+} activities and the added amount of $\text{Cu}(\text{NO}_3)_2$ in the presence of plain
466 polystyrene fluorescent microspheres, Figure S3 of relationships between the percentage of
467 dissolved amount of one compound and the added amount of other compounds in mixtures,
468 Table S1 of the experimental set up for mixtures, Table S2 of particle characterization by
469 dynamic light scattering. This information is available free of charge via the Internet at
470 <http://pubs.acs.org/>.

471 **References**

- 472 (1) Rousk, J.; Ackermann, K.; Curling, S. F.; Jones, D. L. Comparative toxicity of
473 nanoparticulate CuO and ZnO to soil bacterial communities. *PLoS one* **2012**, *7*, e34197.
- 474 (2) Mortimer, M.; Kasemets, K.; Kahru, A. Toxicity of ZnO and CuO nanoparticles to ciliated
475 protozoa *Tetrahymena thermophila*. *Toxicology* **2010**, *269* (2), 182-189.

- 476 (3) Misra, S. K.; Dybowska, A.; Berhanu, D.; Luoma, S. N.; Valsami-Jones, E. The
477 complexity of nanoparticle dissolution and its importance in nanotoxicological studies. *Sci.*
478 *Total Environ.* **2012**, *438*, 225-232.
- 479 (4) Franklin, N. M.; Rogers, N. J.; Apte, S. C.; Batley, G. E.; Gadd, G. E.; Casey, P. S.
480 Comparative toxicity of nanoparticulate ZnO, bulk ZnO, and ZnCl₂ to a freshwater microalga
481 (*Pseudokirchneriella subcapitata*): the importance of particle solubility. *Environ. Sci. Technol.*
482 **2007**, *41* (24), 8484-8490.
- 483 (5) Borm, P.; Klaessig, F. C.; Landry, T. D.; Moudgil, B.; Pauluhn, J.; Thomas, K.; Trottier, R.;
484 Wood, S. Research strategies for safety evaluation of nanomaterials, part V: role of
485 dissolution in biological fate and effects of nanoscale particles. *Toxicol. Sci.* **2006**, *90* (1), 23-
486 32.
- 487 (6) Adamson, A. W.; Gast, A. P. *Physical chemistry of surfaces*; Wiley Press: New York,
488 U.S., 1997.
- 489 (7) Holsapple, M. P.; Farland, W. H.; Landry, T. D.; Monteiro-Riviere, N. A.; Carter, J. M.;
490 Walker, N. J.; Thomas, K. V. Research strategies for safety evaluation of nanomaterials, part
491 II: toxicological and safety evaluation of nanomaterials, current challenges and data needs.
492 *Toxicol. Sci.* **2005**, *88* (1), 12-17.
- 493 (8) Ribeiro, F.; Gallego-Urrea, J. A.; Goodhead, R. M.; Van Gestel, C. A.; Moger, J.; Soares,
494 A. M.; Loureiro, S. Uptake and elimination kinetics of silver nanoparticles and silver nitrate by
495 *Raphidocelis subcapitata*: The influence of silver behaviour in solution. *Nanotoxicology* **2014**,
496 *9* (6), 686-695.
- 497 (9) Blinova, I.; Ivask, A.; Heinlaan, M.; Mortimer, M.; Kahru, A. Ecotoxicity of nanoparticles of
498 CuO and ZnO in natural water. *Environ. Pollut.* **2010**, *158* (1), 41-47.
- 499 (10) Bondarenko, O.; Ivask, A.; Käkinen, A.; Kahru, A. Sub-toxic effects of CuO
500 nanoparticles on bacteria: Kinetics, role of Cu ions and possible mechanisms of action.
501 *Environ. Pollut.* **2012**, *169*, 81-89.
- 502 (11) Ivask, A.; Juganson, K.; Bondarenko, O.; Mortimer, M.; Aruoja, V.; Kasemets, K.;
503 Blinova, I.; Heinlaan, M.; Slaveykova, V.; Kahru, A. Mechanisms of toxic action of Ag, ZnO

- 504 and CuO nanoparticles to selected ecotoxicological test organisms and mammalian cells in
505 vitro: A comparative review. *Nanotoxicology* **2013**, *8* (sup1), 57-71.
- 506 (12) Fernández-Cruz, M. L.; Lammel, T.; Connolly, M.; Conde, E.; Barrado, A. I.; Derick, S.;
507 Perez, Y.; Fernandez, M.; Furger, C.; Navas, J. M. Comparative cytotoxicity induced by bulk
508 and nanoparticulated ZnO in the fish and human hepatoma cell lines PLHC-1 and Hep G2.
509 *Nanotoxicology* **2013**, *7* (5), 935-952.
- 510 (13) Song, L.; Connolly, M.; Fernández-Cruz, M. L.; Vijver, M. G.; Fernández, M.; Conde, E.;
511 de Snoo, G.; Peijnenburg, W. J., Navas, J. M. Species-specific toxicity of copper
512 nanoparticles among mammalian and piscine cell lines. *Nanotoxicology* **2014**, *8* (4), 383-393.
- 513 (14) Karlsson, H. L.; Gliga, A. R.; Calléja, F. M.; Gonçalves, C. S.; Wallinder, I. O.; Vrieling,
514 H.; Fadeel, B.; Hendriks, G. Mechanism-based genotoxicity screening of metal oxide
515 nanoparticles using the ToxTracker panel of reporter cell lines. *Part. Fibre. Toxicol.* **2014**, *11*
516 (1), 1-14.
- 517 (15) Kahru, A.; Dubourguier, H. C. From ecotoxicology to nanoecotoxicology. *Toxicology*
518 **2010**, *269* (2), 105-119.
- 519 (16) Bystrzejewska-Piotrowska, G.; Golimowski, J.; Urban, P. L. Nanoparticles: their
520 potential toxicity, waste and environmental management. *Waste Manage.* **2009**, *29* (9),
521 2587-2595.
- 522 (17) Bolyard, S. C.; Reinhart, D. R.; Santra, S. Behavior of engineered nanoparticles in
523 landfill leachate. *Environ. Sci. Technol.* **2013**, *47* (15), 8114-8122.
- 524 (18) Li, L.; Fernández-Cruz, M. L.; Connolly, M.; Conde, E.; Fernández, M.; Schuster, M.;
525 Navas, J. M. The potentiation effect makes the difference: Non-toxic concentrations of ZnO
526 nanoparticles enhance Cu nanoparticle toxicity in vitro. *Sci. Total Environ.* **2015**, *505*, 253-
527 260.
- 528 (19) Batley, G. E.; Kirby, J. K.; McLaughlin, M. J. Fate and risks of nanomaterials in aquatic
529 and terrestrial environments. *Accounts Chem. Res.* **2012**, *46* (3), 854-862.
- 530 (20) Hong, J.; Rico, C. M.; Zhao, L.; Adeleye, A. S.; Keller, A. A.; Peralta-Videa, J. R.;
531 Gardea-Torresdey, J. L. Toxic effects of copper-based nanoparticles or compounds to

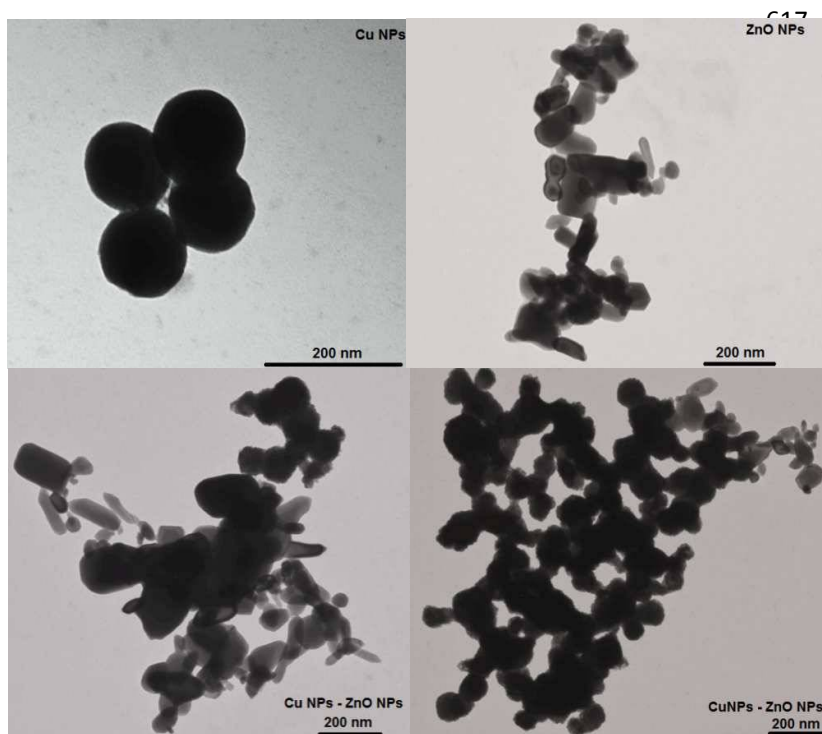
- 532 lettuce (*Lactuca sativa*) and alfalfa (*Medicago sativa*). *Environ. Sci. Processes Impacts* **2015**,
533 17, 177-185.
- 534 (21) Rico, C.M.; Majumdar, S.; Duarte-Gardea, M.; Peralta-Videa, J. R.; Gardea-Torresdey,
535 J. L. Interaction of nanoparticles with edible plants and their possible implications in the food
536 chain. *J. Agr. Food. Chem.* **2011**, 59, 3485-3498.
- 537 (22) Hu, C. W.; Li, M.; Cui, Y. B.; Li, D. S.; Chen, J.; Yang, L. Y. Toxicological effects of TiO₂
538 and ZnO nanoparticles in soil on earthworm *Eisenia fetida*. *Soil Biol. Biochem.* **2010**, 42 (2),
539 586-591.
- 540 (23) Song, W.; Zhang, J.; Guo, J.; Zhang, J.; Ding, F.; Li, L.; Sun, Z. Role of the dissolved
541 zinc ion and reactive oxygen species in cytotoxicity of ZnO nanoparticles. *Toxicol. Lett.* **2010**,
542 199 (3), 389-397.
- 543 (24) Le, T. T. Y.; Vijver, M. G.; Jan Hendriks, A.; Peijnenburg, W. J. Modeling toxicity of
544 binary metal mixtures (Cu²⁺-Ag⁺, Cu²⁺-Zn²⁺) to lettuce, *Lactuca sativa*, with the biotic ligand
545 model. *Environ. Toxicol. Chem.* **2013**, 32 (1), 137-143.
- 546 (25) Liu, Y.; Vijver, M. G.; Peijnenburg, W. J. Comparing three approaches in extending
547 biotic ligand models to predict the toxicity of binary metal mixtures (Cu-Ni, Cu-Zn and Cu-
548 Ag) to lettuce (*Lactuca sativa* L.). *Chemosphere* **2014**, 112, 282-288.
- 549 (26) Cedergreen, N.; Sørensen, H.; Svendsen, C. Can the joint effect of ternary mixtures be
550 predicted from binary mixture toxicity results? *Sci. Total. Environ.* **2012**, 427, 229-237.
- 551 (27) *OECD Test Guidelines 208: Terrestrial plant test-seedlings emergence and seedling*
552 *growth test*; OECD Guidelines for the Testing of Chemicals; Organization for Economic Co-
553 operation and Development: Paris, 2006.
- 554 (28) *Protocols for short term toxicity screening of hazardous waste sites*; EPA 600/3-88/029;
555 United States Environmental Protection Agency: Washington, DC, 1988.
- 556 (29) Pfleeger, T.; Mc Farlane, C.; Sherman, R.; Volk, G. Short-term bioassay for whole plant
557 toxicity. In *Plants for toxicity assessment*; Gorsuch, J. W., Lower, W. R., Lewis, M. A., Wang,
558 W. C., Eds.; American Society for Testing and Materials Press: Philadelphia 1991; 355-364.
- 559 (30) Bliss, C. I. The toxicity of poisons applied jointly. *Ann. Appl. Biol.* **1939**, 26 (3), 585-615.

- 560 (31) Berenbaum, M. C. The expected effect of a combination of agents: the general solution.
561 *J. Theor. Biol.* **1985**, *114*, 413-431.
- 562 (32) Loewe, S.; Muischnek, H. Uber die Kombinationswirkungen. 1. Mitteilung: Hilfsmittel der
563 Fragestellung. *Naunyn. Schmiedebergs Arch. Exp. Pathol. Pharmacol.* **1926**, *114*, 313-326.
564 (German)
- 565 (33) *Harmonisation of human and ecological risk assessment of combined exposure to*
566 *multiple chemicals*; EFSA Supporting publication EN-784; European Food Safety Authority:
567 Edinburgh, 2015.
- 568 (34) Sprague, J. B. Measurement of pollutant toxicity to fish. II. Utilizing and applying
569 bioassay results. *Water Research* **1970**, *4*, 3-32.
- 570 (35) Thakali, S.; Allen, H. E.; Di Toro, D. M.; Ponizovsky, A. A.; Rooney, C. P.; Zhao, F. J.;
571 McGrath, S. P. A terrestrial biotic ligand model. 1. Development and application to Cu and Ni
572 toxicities to barley root elongation in soils. *Environ. Sci. Technol.* **2006**, *40*, 7085-7093.
- 573 (36) Sharma, S. S.; Schat, H.; Vooijs, R.; Van Heerwaarden, L. M. Combination toxicology of
574 copper, zinc, and cadmium in binary mixtures: concentration-dependent antagonistic,
575 nonadditive, and synergistic effects on root growth in *Silene Vulgaris*. *Environ. Toxicol.*
576 *Chem.* **1999**, *18* (2), 348-355.
- 577 (37) Li, M.; Lin, D.; Zhu, L. Effects of water chemistry on the dissolution of ZnO nanoparticles
578 and their toxicity to *Escherichia coli*. *Environ. Pollut.* **2013**, *173*, 97-102.
- 579 (38) Lee, W. M.; An, Y. J.; Yoon, H.; Kweon, H. S. Toxicity and bioavailability of copper
580 nanoparticles to the terrestrial plants mung bean (*Phaseolus radiatus*) and wheat (*Triticum*
581 *aestivum*): plant agar test for water-insoluble nanoparticles. *Environ. Toxicol. Chem.* **2008**,
582 *27* (9), 1915-1921.
- 583 (39) Remans, T.; Thijs, S.; Truyens, S.; Weyens, N.; Schellingen, K.; Keunen, E.; Gielen, H.;
584 Cuypers, A.; Vangronsveld, J. Understanding the development of roots exposed to
585 contaminants and the potential of plant-associated bacteria for optimization of growth. *Ann.*
586 *Bot.* **2012**, *110*, 239-252.

- 587 (40) Ali, N. A.; Bernal, M. P.; Ater, M. Tolerance and bioaccumulation of copper in
588 *Phragmites australis* and *Zea mays*. *Plant Soil* **2002**, 239, 103-111.
- 589 (41) Le, T. T. Y.; Vijver, M. G.; Kinraide, T. B.; Peijnenburg W. J. G. M. Modelling metal-
590 metal interactions and metal toxicity to lettuce *Lactuca sativa* following mixture exposure
591 (Cu^{2+} - Zn^{2+} and Cu^{2+} - Ag^{+}). *Environ. Pollut.* **2013**, 176, 185-192.
- 592 (42) Liu, Y.; Vijver, M. G.; Qiu, H.; Baas, J.; Peijnenburg, W. J. G. M. Statistically significant
593 deviations from additivity in metal mixtures, what do they mean? *Ecotox. Environ. Safe.* **2015**,
594 122, 37-44.
- 595 (43) Qiu, A.; Hogstrand, C. Functional expression of a low-affinity zinc uptake transporter
596 (FrZIP2) from pufferfish (*Takifugu rubripes*) in MDCK cells. *Biochem. J.* **2005**, 390 (Pt 3),
597 777-786.
- 598
- 599
- 600
- 601
- 602
- 603
- 604
- 605
- 606
- 607
- 608
- 609
- 610
- 611
- 612
- 613
- 614

615

616



626 Figure 1. TEM images of Cu NPs, ZnO NPs and their mixtures (prepared in lettuce culture
627 medium). Scale bars indicate size (nm).

628

629

630

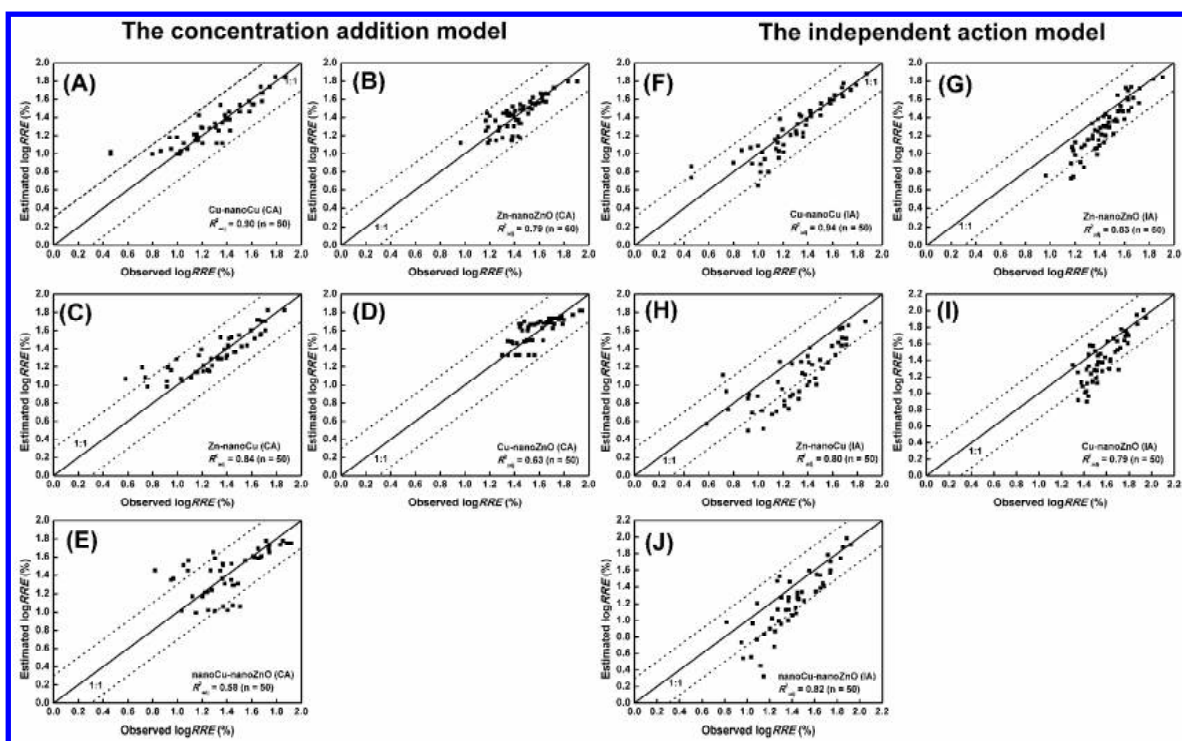
631

632

633

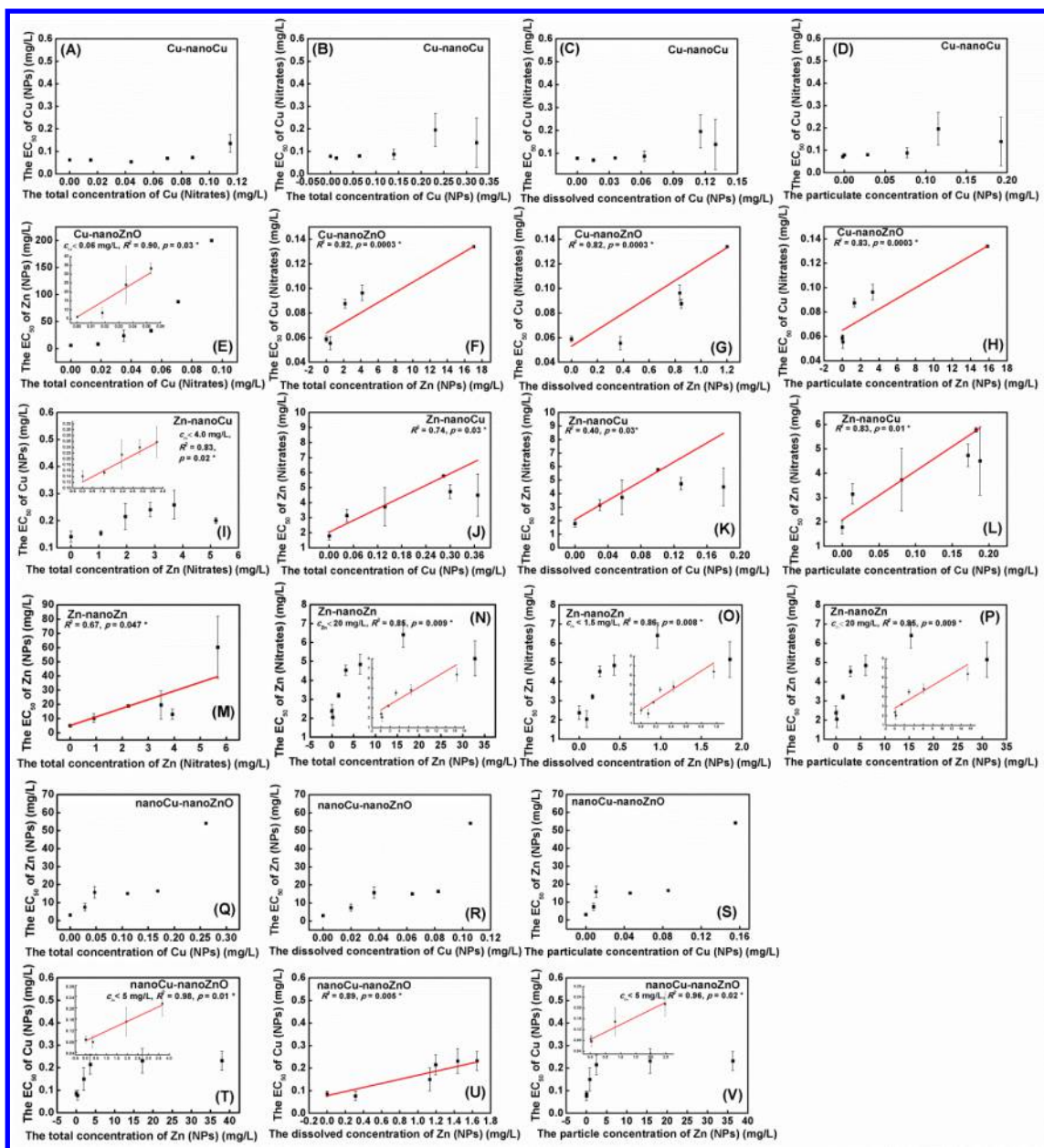
634

635



636

637 Figure 2. Relationships between the observed and estimated log 4-d relative root elongation
 638 (RRE , %) of Cu-nanoCu, Zn-nanoZnO, Cu-nanoZnO, Zn-nanoCu and nanoCu-nanoZnO
 639 mixtures for lettuce *Lactuca sativa* L. using the CA model (A-E) and the IA model (F-J). R^2_{adj}
 640 indicates the adjusted determination coefficient. n indicates the number of data points. The
 641 solid line represents the perfect fit (1:1 line) and the dotted lines represent a difference of a
 642 factor of 2 between the observed and estimated values.



643

644 Figure 3. Relationships between the median effective concentrations (EC_{50} s) of one
 645 component for *L. sativa* L. after 4-d exposure and the concentration (total, dissolved,
 646 particulate) of the other components in mixtures of Cu-nanoCu, Zn-nanoZnO, Cu-nanoZnO,
 647 Zn-nanoCu, nanoCu-nanoZnO. Data are presented as mean \pm standard error of the mean.
 648 Solid lines represent the statistically significant linear fits (a positive slope indicates an
 649 overall antagonistic effects; a negative slope indicates an overall synergistic effects). The
 650 smaller graphs inside figures depict significant effects occurring at low concentration levels.

651 The dissolved concentrations of metal-based NPs were expressed as the average value
652 after 1 h and 24 h of equilibration. R^2 indicates the determination coefficient adjusted for the
653 degrees of freedom. p indicates the statistical significance level. * indicates that the slope of
654 linear curve is significantly different from zero at the 5% significance level.

655

656

657

658

659

660

661

662

663

664

665

666

667

668

669

670

671

672 Table 1. The median effective concentrations (EC_{50} , mg/L) or median effective activities
 673 (EA_{50} , $\mu\text{mol/L}$) with the standard error of the mean (SEM) or the 95% confidence interval (CI)
 674 of Cu NPs, ZnO NPs, $\text{Cu}(\text{NO}_3)_2$ and $\text{Zn}(\text{NO}_3)_2$ individually on 4-d root elongation of lettuce (*L.*
 675 *sativa* L.) in the present study and in the previous study.

Compounds	Metal species	EC_{50} (mg/L) or EA_{50} ($\mu\text{mol/L}$)	n	Sources
Cu NPs	Total Cu	0.10 (± 0.01)	7	This study
ZnO NPs	Total Zn	4.47 (± 0.62)	7	This study
$\text{Cu}(\text{NO}_3)_2$	Dissolved Cu	0.07 (± 0.006)	4	This study
$\text{Zn}(\text{NO}_3)_2$	Dissolved Zn	2.08 (± 0.25)	4	This study
$\text{Cu}(\text{NO}_3)_2$	Cu^{2+}	0.03 (0.02 ~ 0.04)	-	24
$\text{Zn}(\text{NO}_3)_2$	Zn^{2+}	106 (91.1 ~ 124)	-	24

676 n: the number of replicates; -: not determined.

677

678

679

680

681

682

683

684

685

686

687

688 Table 2. Fitting results of the toxicity of Cu-Zn, Cu-nanoCu, Zn-nanoZnO, Cu-nanoZnO, Zn-nanoCu, and nanoCu-nanoZnO mixtures by the
689 concentration addition (CA) model and the independent action (IA) model.

Mixtures	The IA model		The CA model				Sources
	R^2_{adj}	p value	R^2_{adj}	p value	$TU_{mix}^{50\%}$ (\pm SE)	β (\pm SE)	
Cu-Zn (n=122)	0.92	<0.0001*	0.92	<0.0001*	-	-	41
Cu-nanoCu (n=50)	0.94	<0.0001*	0.90	<0.0001*	0.79 (\pm 0.04)	1.34 (\pm 0.07)	This study
Zn-nanoZnO (n=60)	0.83	<0.0001*	0.79	<0.0001*	0.92 (\pm 0.08)	0.79 (\pm 0.06)	This study
Cu-nanoZnO (n=50)	0.79	<0.0001*	0.63	<0.0001*	1.16 (\pm 0.13)	0.62 (\pm 0.07)	This study
Zn-nanoCu (n=50)	0.80	<0.0001*	0.84	<0.0001*	1.44 (\pm 0.07)	1.65 (\pm 0.12)	This study
nanoCu-nanoZnO (n=50)	0.82	<0.0001*	0.58	<0.0001*	0.81 (\pm 0.11)	0.88 (\pm 0.12)	This study

690 R^2_{adj} : the adjusted coefficient of determination; p : the outcome of the likelihood ratio test; *: significant at the 5% significance level; β : the shape
691 parameter that determines the steepness of the response curves; $TU_{mix}^{50\%}$: the sum of toxic units of a mixture inducing 50% inhibition of root
692 elongation; SE: standard error; -: not determined; n: the number of data points.

693

694 Table 3. Mutual impacts found between mixture components in combinations of Cu-Zn, Cu-nanoCu, Zn-nanoZnO, Cu-nanoZnO, Zn-nanoCu,
695 and nanoCu-nanoZnO in the exposure of 4-d lettuce seedlings.

Substance 1 Substance 2	Zn (NO ₃) ₂	Cu (NO ₃) ₂	Cu NPs	Dissolved Cu	Particulate Cu
	Cu (NO ₃) ₂	Anta\Anta ^{24,25}	n.d.	No\No	No\n.d.
Zn (NO ₃) ₂	n.d.	Anta\Anta ^{24,25}	Anta\No	Anta\n.d.	Anta\n.d.
ZnO NPs	Anta\Anta	Anta\Anta	No\Anta	No\n.d.	No\n.d.
Dissolved Zn	n.d.\Anta	n.d.\Anta	n.d.\Anta	n.d.	n.d.
Particulate ZnO	n.d.\Anta	n.d.\Anta	n.d.\Anta	n.d.	n.d.

696 No significant effect (No): the slope of the linear fits in Figure 3 is not significantly different from zero, which indicates that no significant effects
697 of one component were observed on the EC₅₀ values of another component; Antagonism (Anta): the positive slope of linear fits in Figure 3
698 significantly deviates from zero ($p < 0.05$), which indicates an antagonistic effect of one component on another component in the mixture; n.d.:
699 not detected in this study; \: the left side indicates the effects of Substance 1 on Substance 2 and the right side indicates the effects of
700 Substance 2 on Substance 1.